International Journal of Innovative Technology and Exploring Engineering (IJITEE)
ISSN: 2278-3075 (Online), Volume-9 Issue-4, February 2020

Free Vibration Response of Four-Parameter Functionally Graded Thick Spherical Shell Formulation on FEA

Raparthi Srilakshmi, Ch. Ratnam, Chandra Mouli Badiganti

Abstract: ***The following study explored the free vibration characteristics of a rectangular spherical shell. An efficient formulation developed Higher-order shear deformation theory (HSDT), conjunction with the numerical procedure (FEM). To determine the desired volume fraction obtained through the Four-parameter power-law distribution considered on the top surface is ceramic-rich. In contrast, the base surface is metal-rich. Parameters distribution gives design flexibility and different kinds of material profiles exhibited. The efficiency of the model is verified by performing convergence studies and comparison tests. The numerical results compared with earlier available literature solutions to authenticate the stability and exactness of the current approach, and good agreement perceived. Illustrated numerical examples to find the influence on the appropriate selection of the four-parameters, the mechanical behavior of the composition and effects on geometrical parameters, skew angles, different boundary conditions on their non-dimensional frequency responses examined in detail***.

Keywords:Free vibration,skew angle, Finite element method,Spherical shell.

I. INTRODUCTION

Material is a fundamental ingredient in the design of complex structures in many engineering applications. They withstand complicated environmental conditions, which is the present-day requirement to produce high-performance characteristic materials. In the last two decades, several researchers focused on Functionally Graded Structural materials (FGMs). FGMs are a new class of composites materials made from a mixture of ceramic and metal, which resulted in the production of structural elements like Plates, Shells, and Beams. Their composition varies with a continuous change in the volume fraction of constituent through-thickness direction. FGM has a tremendous advantage of being able to resist high temperatures while maintaining structural integrity. Shells are essential structural elements because of their load-carrying capacity and extensive usage in space applications and dome-shaped structures like aircraft, pressure vessels, and nuclearcontainment structures.

Revised Manuscript Received on February 28, 2020.
***** Correspondence Author
Raparthi Srilakshmi*, Department of Mechanical Engineering, Andhra University, Visakhapatnam, India. Email: srilakshmi053@gmail.com
Ch. Ratnam, Department of Mechanical Engineering, Andhra University, Visakhapatnam, India. Email: chratnam@gmail.com
Chandra Mouli Badiganti, Department ofMechanical Engineering, RISE Group ofInstitutions, Ongole, India. Email: badiganti1@gmail.com

Investigations on free vibration characteristics of FG spherical shells and its limited literature availability is an exciting field for study in recent years.FGMs was first introduced in 1984/1987 by a group of Japanese material scientists [1].

Loy et al. [2] investigated the vibration of cylindrical shells made of functionally graded stainless steel and nickel materials by Considering simply supported boundary conditions. The analysis examined with Based-on Love's Shell theory and Rayleigh-Ritz's method. They identified that the natural frequency is affected by the constituent volume fraction and the configurations of the constituent materials. In the same way Pradhan et al. [3] studied FG Cylindrical Shells under different boundary conditions. Reddy [4] presented the analysis of functionally graded plates based on the TSDT.

Y.S. Lee et al. [5] presented the free vibration characteristics of joined spherical -cylindrical shells with different classical boundary conditions. The detailed parametric studies scrutinized on the effect of the shallowness of the spherical and length of the cylindrical shell structures. J.N. Reddy and Z.Q. Cheng [6] examined a functionally graded spherical shallow shell in polygonal planform based on the classical theory and the first order and third-order shear deformation theories. The Mori Tanaka scheme used to estimate the material properties. Patel et al. [7] presented the free vibration behavior of elliptical cylindrical F.G. shells based on higher-order shear deformation theory and employing the finite element method. The significance of various parameters and mode shapes on non-circular cross-sections are studied.Hu et al. [8] studied a numerical method for free vibration of a rotating twisted and open conical shell is presented by the energy method.

Xiang et al. [9] presented to study the vibration behavior of the ring supported cylindrical shells based on the Thin shell Goledenveizer-Novazhilov theory. Woo et al. [10] presented, the post-buckling behavior of moderately thick FG plates and shallow cylindrical shells under edge compressive and thermal loadings is studied. E. Artioli and Viola [11] presented the free vibration analysis of spherical caps formulation on genialized differential quadrature method and First-order shear deformation theory.

Arciniega and J.N. Reddy [12] examined, Nonlinear analysis for functionally graded shells using first-order shear deformation theory.Zhao et al. [13]-[15] analyzed the free vibration of functionally graded cylindrical and conical shell panels and plates using the element-free KP-Ritz method and using FSDT.

F. Tornabene and E. Viola [16]-[17] developed based on numerical method (G.D.Q) the dynamic behavior of vibration analysis of hemispherical domes and spherical shell panels. Later on, with the same method the author's developed a 2-D solution for free vibrations of parabolic shells using the First-order Shear Deformation Theory (FSDT)compared different commercial courses such as Abaqus, Ansys, Femap/Nastran, Straus, Pro/Mechanica Numerical solutions analyzed. F. Tornabene [18] investigated numerical study on dynamic behavior of moderately thick functionally graded conical, cylindrical shells and annular plates with two different power-law distributions and using FSDT and GDQ approach.

Tornabene et al. [19]– [21] proposed to determine the response of various structures, the generalized differential quadrature method approach continued. The free vibration analysis of functionally graded parabolic panel with the three-parameter power-law distribution. Later on, doubly curved shells and panels with four-parameter power-law delivery examined.

M.H.yas and B. Sobhani Aragh [22] studied three-dimensional analysis of FG fiber-reinforced cylindrical panel. Shen and Z.X. Wang [23] presented comparison studies that reveal two kinds of micromechanics models, namely Mori-Tanaka and Voigt's and models for vibration analysis of FG plates.

Neves A.M.A et al. [24] presented the Unified Formulation applied based on HSDT with free vibration problems of functionally graded thin and thick cylindrical, spherical shell panels.V. R. Kar and S. K. Panda [25] Investigated the free vibration characteristics of FG single/double curved panels different geometries under linear and nonlinear, the behavior of temperatures regions presented.

Kumar et al. [26] proposed a free Vibration analysis of laminated skew composite cylindrical shells. A C_0 finite element formulation and the isoperimetric element associated with HSDT.

Wang et al. [27] provided an FSDT based procedure on vibration analysis for the four-parameter functionally graded moderately thick doubly curved shells and panels of revolution with general boundary conditions.Devesh Punera and Tarun Kant [28] developed Free vibration of FG open cylindrical shells based on numerous refined higher-order displacement models.

Computed fundamental natural frequency on geometric parameters and material gradation scrutinized. Mouli and Ramji Koona [29], [30] analyzed the influence of different parameters on the free vibration behavior r of FG Skew shallow curved panels.

The present paper is focused on the free vibration characteristics of FG rectangular spherical shell. The formulation is based on Higher-order deformation theory conjunction with the finite-element method.

The main contribution of this work is to illustrate the influence of skew angle, power-law exponent, four parameter power-law distributions and choice of four parameters on material composition in terms of volume fraction constituents, Geometric parameters aspect ratio, thickness ratio, and curvature ratio, the effect of different boundary conditions under the non-dimensional frequency responses, The current model is applied in the solution of some illustrative examples and the results arepresented and discussed.

II. VOLUME FRACTION PROFILES

In this section, to initiate new generalized power-law distribution for specifying variation of volume fraction in FGM composites. By using four-parameter power-law delivery, it is possible to study the effect of the different kinds of material profiles incorporate varying the values of power-law exponent with classical, Symmetric, and asymmetric volume fraction profiles on the mechanical behavior of the FGM structure. In which subscripts c and m represent the ceramic and metal constituents, whereV_c and V_m are the volume fractions of ceramic and metal respectively, Refer to (1a), (1b), and (1c) mechanical properties are Young's modulus E(ξ), density(ξ), and poisons ratio(ν) expressed in the form of a linear combination. The sum of the volume fraction of the constituent materials should be equal to one, Refer to(2).

$$\mathrm{E}(\xi) = (E_c - E_m)V_c + V_m \qquad (1a)$$

$$\rho(\xi) = (\rho_c - \rho_m)V_c + \rho_m \qquad (1b)$$

$$\nu(\xi) = (V_c - V_m)V_c + \nu_m \qquad (1c)$$

$$V_c + V_m = 1 \qquad (2)$$

The four parameters are represented by u, v, w,φ and total thickness of the shell is (h), Where φ is the power-law exponent varying as $0 \le \varphi \le \infty$. For example, the material distribution in the FGM shell is continuously varied, such that the bottom surface (-h/2) of the structure is rich in metal. In contrast, the top surface (+h/2) is rich in ceramic, by setting u = 1 and v = 0, w=0, Refer to(3)

$$\mathrm{FGM}_{(u/v/w/\varphi)}: \mathrm{V}_C = \left(1 - u\left(\frac{1}{2} - \frac{\xi}{h}\right) + \mathrm{v}\left(\frac{1}{2} - \frac{\xi}{h}\right)^{w}\right)^{\varphi} \qquad (3)$$

Fig.1 shows the four-parameter power law distribution can be attained by setting relevant value of the parameters u, v, w, andφ. the variation of the ceramic volume fraction for various values of the parameters u, v, w, φ are described. classic volume fraction profiles, power-law distributions are considered for the volume fraction of the ceramic.The first distribution FGM (u=1, v=0/w=1/φ), the material composition is continuously varied, such that the top surface(ξ/h=0.5) is ceramic-rich.In contrast, the bottom surface of ξ/h=-0.5 of the shell's metal-rich.

Fig.2 shows the significance of the various power-law distribution of patterns by modifying the parameters u, v, w, and φ for the given constituents of volume fraction.by varying the power law exponent (φ) and symmetric respect to the reference surface (ξ/h=0) of the shell.by setting the first four parameter power law distribution FGM (u=1,v=1 and w=3).

Fig.3 illustrate profiles are not symmetric with respect to the reference surface (ξ/h=0) of theshell. asymmetric profiles obtained by setting FGM (u=1, v=1, w=5/φ).

Fig. 1-6. Variation of ceramic volume fraction (V_c)through the functionally graded structure thickness(ξ) for different values of three parameters u, v, w and power-law gradient exponent (φ)

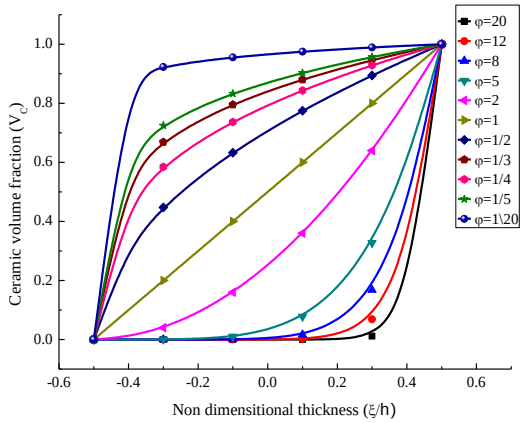

Fig 1.FGM(u=1/v=0/w=1/φ)

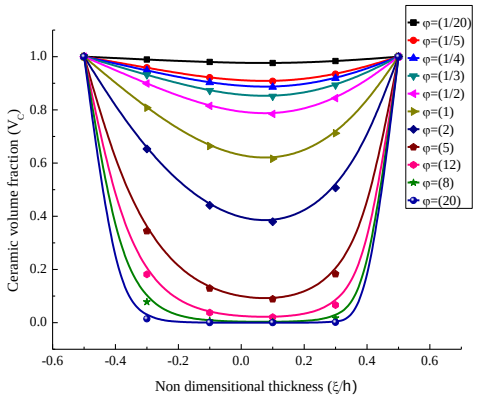

Fig 2. FGM(u=1/v=1/w=3/φ)

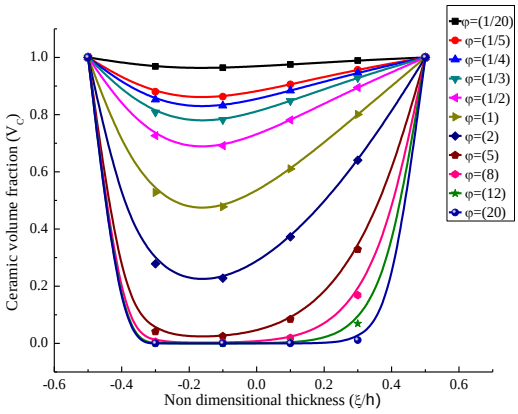

Fig 3. FGM(u=1/v=1/w=5/φ)

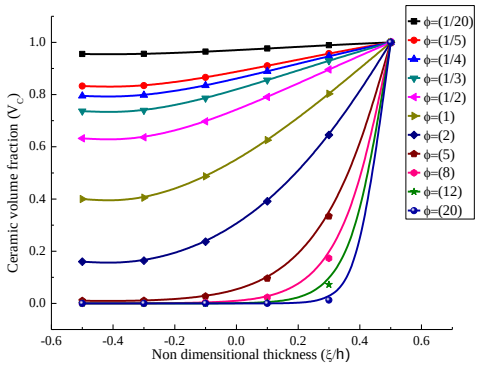

Fig 4. FGM(u=1/v=0.4/w=3/φ)

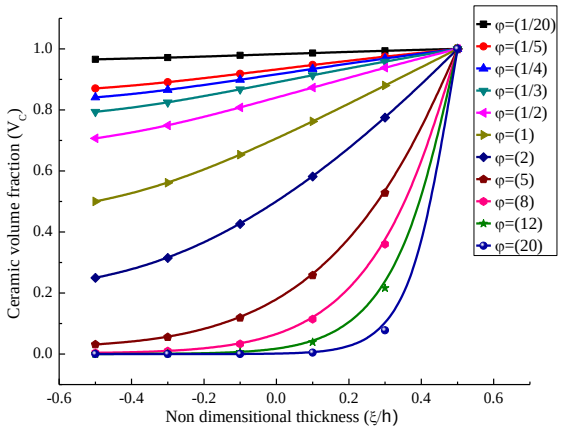

Fig1. 1 Fig 5. FGM(u=0.6/v=0.1/w=1/φ)

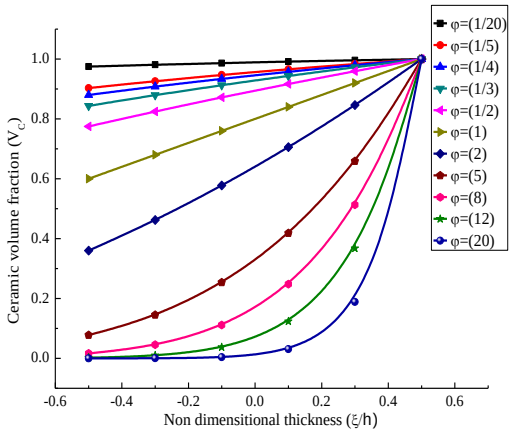

Fig 6. FGM(u=0.4/v=0/w=1/φ)

Figs.4-6. depicts other cases obtained by varying the parameters u, v, w. These material profiles characterized by the fact that one of the shells surfaces the top or bottom surface presents a composed of two constituents.

For example, by setting the values as in (3) and the power-law distribution is FGM (u=1, v=0.4, w=3) and different quantity values of the power-law exponent.

From the design point of view, it is essential to know the top surface is of the shell ξ/h=0.5 is ceramic or metal. If the bottom surface ξ/h=-0.5 is metal or ceramic- rich. Or One of these surfaces presents a mixture of two constituents. It is worth noting that four-parameter power-law distributions as given by F. Tornabene [18], and the author provided more detailed description about the material variation profile of FGMs.

The main objective of this study examines the effect of the volume fraction of the material constituents. The four-parameter power-law distribution on the parametric response. the Voigt's rule is employed to evaluate the active. Thus, material properties of layers varying continuously and smoothly in the thickness direction.The Influence of choice of the material parameters u, v, w, and Power-law exponent (φ), different boundary conditions, geometrical parameters, and the effect of skew angles on the non- dimensional natural frequency investigated. The Influence of this study provided various kinds of material pattern profiles, the classic, symmetric, asymmetric effects on the mechanical behavior of a structure.

III. FRAMEWORK OF GOVERNING EQUATIONS

A. Kinematic Paradigm and numerical procedure

In the present study, a general shallow curved spherical shell is represented by a, b, and thickness h, in x, y directions, as shown in Fig.7. Here, Rx and Ry are the radii of curvature along x and y orientation, respectively. The TSDT mid-plane kinematics model utilized to define the globaldisplacements ($\chi,\lambda,\psi,$) at any point in terms of mid-plane displacements (χ_0, λ_0, ψ_0), rotations (θ_x, θ_y) and higher-order ($\chi_0^*, \lambda_0^*, \theta_x^*, \theta_y^*$) terms, as per Pandya & Kant, [32].

$$\left.\begin{aligned}\chi &= \chi_0 + \xi\theta_x + \xi^2\chi_0^* + \xi^3\theta_x^*\\ \lambda &= \lambda_0 + \xi\theta_y + \xi^2\lambda_0^* + \xi^3\theta_y^*\\ \psi &= \psi_0\end{aligned}\right\} \qquad (4)$$

This kinematic model, (4) can be rewritten in the matrix form Refer to(5)

$$\{\delta\} = [F]\{\delta_0\} \qquad (5)$$

Where $\{\delta\} = \lfloor\chi \quad \lambda \quad \psi\rfloor^T$ and $\{\delta_0\} = \lfloor\chi_0 \quad \lambda_0 \quad \psi_0 \quad \theta_x \quad \theta_y \quad \chi_0^* \quad \lambda_0^* \quad \theta_x^* \quad \theta_y^*\rfloor^T$ are the global and mid-plane displacement vectors. $[F]$ contains the thickness coordinate functions, as expressed here, Refer to (6)

$$[F] = \begin{bmatrix}1 & 0 & 0 & \xi & 0 & \xi^2 & 0 & \xi^3 & 0\\ 0 & 1 & 0 & 0 & \xi & 0 & \xi^2 & 0 & \xi^3\\ 0 & 0 & 1 & 0 & 0 & 0 & 0 & 0 & 0\end{bmatrix} \qquad (6)$$

The shallow curved shell is shown in Fig.7(ii) with sides *a* and *b*. To constraint the oblique edges, the local displacement vector is required to transform to global via transformation matrix [*F* and expressed in cosine (*l*) and sine (*m*) terms. The displacement transformation revealed as

$$\begin{Bmatrix}\chi_0\\ \lambda_0\\ \psi_0\\ \theta_x\\ \theta_y\\ \chi_0^*\\ \lambda_0^*\\ \theta_x^*\\ \theta_y^*\end{Bmatrix}\begin{bmatrix}l & -m & 0 & 0 & 0 & 0 & 0 & 0 & 0\\ m & l & 0 & 0 & 0 & 0 & 0 & 0 & 0\\ 0 & 0 & 1 & 0 & 0 & 0 & 0 & 0 & 0\\ 0 & 0 & 0 & l & -m & 0 & 0 & 0 & 0\\ 0 & 0 & 0 & m & l & 0 & 0 & 0 & 0\\ 0 & 0 & 0 & 0 & 0 & l & -m & 0 & 0\\ 0 & 0 & 0 & 0 & 0 & m & l & 0 & 0\\ 0 & 0 & 0 & 0 & 0 & 0 & 0 & l & -m\\ 0 & 0 & 0 & 0 & 0 & 0 & 0 & m & l\end{bmatrix}\begin{Bmatrix}\chi_0'\\ \lambda_0'\\ \psi_0'\\ \theta_x'\\ \theta_y'\\ \chi_0^{*\prime}\\ \lambda_0^{*\prime}\\ \theta_x^{*\prime}\\ \theta_y^{*\prime}\end{Bmatrix} \qquad (10)$$

(7) can also be written as

$$\{\Omega_0\} = [F]\{\Omega_0'\} \qquad (8)$$

where, $\{\Omega_0'\}$ is the displacement field defined in the local coordinates. The strain-displacement equation for any general shallow thick plate can be written as (Kar and Panda, [25])

$$\begin{Bmatrix}\varepsilon_{xx}\\ \varepsilon_{yy}\\ \gamma_{xy}\\ \gamma_{xz}\\ \gamma_{yz}\end{Bmatrix} = \begin{Bmatrix}\frac{\partial\chi}{\partial x} + \frac{\psi}{R_x}\\ \frac{\partial\lambda}{\partial y} + \frac{\psi}{R_y}\\ \frac{\partial\chi}{\partial y} + \frac{\partial\lambda}{\partial x}\\ \frac{\partial\chi}{\partial z} + \frac{\partial\psi}{\partial x} - \frac{\chi}{R_x}\\ \frac{\partial\lambda}{\partial z} + \frac{\partial\psi}{\partial y} - \frac{\lambda}{R_y}\end{Bmatrix} \qquad (9)$$

By imposing the displacement terms (4) in the strain-displacement Refer to (9), the global strain tensor can be modified as

$$\begin{Bmatrix}\varepsilon_{xx}\\ \varepsilon_{yy}\\ \gamma_{xy}\\ \gamma_{xz}\\ \gamma_{yz}\end{Bmatrix} = \begin{Bmatrix}{k_x}^0\\ {k_y}^0\\ {\varepsilon_{xy}}^0\\ {\varepsilon_{xz}}^0\\ {\varepsilon_{yz}}^0\end{Bmatrix} + \xi\begin{Bmatrix}{k_x}^1\\ {k_y}^1\\ {k_{xy}}^1\\ {k_{xz}}^1\\ {k_{yz}}^1\end{Bmatrix} + \xi^2\begin{Bmatrix}{k_x}^2\\ {k_y}^2\\ {k_{xy}}^2\\ {k_{xz}}^2\\ {k_{yz}}^2\end{Bmatrix}\xi^3\begin{Bmatrix}{k_x}^3\\ {k_y}^3\\ {k_{xy}}^3\\ {k_{xz}}^3\\ {k_{yz}}^3\end{Bmatrix} \qquad (10)$$

$$\varepsilon = \varepsilon^0 + \xi k^1 + \xi^2 k^2 + \xi^3 k^3 \qquad (11)$$

where, ε^0, k^1, k^2 and k^3 are the mid-plane strain, curvature and higher-order terms respectively as per Kar and Panda [25].

(11) can be again rearranged as

$$\{\varepsilon\} = [F]\{\bar{\varepsilon}\} \qquad (12)$$

where, $\{\bar{\varepsilon}\} = \lfloor\varepsilon^0 \quad k^1 \quad k^2 \quad k^3\rfloor^T$ is the mid-plane strain, and $F = [I \quad \xi I \quad \xi^2 I \quad \xi^3 I]$ is the thickness-coordinate matrix, in which *I* is the unit matrix of size 5×5.

B.Finite Element Approximations

In this section, the present FG shallow spherical panel is discretized based on a finite element modeling using a nine-node isoperimetric element with eighty-one degrees-of the displacements defined in the mid-plane can in a nodal form as

$$\{\Omega_0\} = \sum_{i=1}^{9} N_i \{\Omega_{0_i}\} \quad (13)$$

where, $\{\Omega_{0_i}\}$ and N_i are the nodal displacement vector and the approximation function at i^{th} node (Cook etal.[31]).

Now, the total and geometric mid-plane strain vectors can be expressed, Refer to(13) as

$$\{\bar{\varepsilon}\} = [B]\{\Omega_{0_i}\} \text{ and } \{\bar{\varepsilon}_G\} = [B_G]\{\Omega_{0_i}\} \quad (14)$$

$$([K] - [K_G] - \omega^2[M])\Delta = 0 \quad (15)$$

where, $[M]=[N]^T[m][N]$ is the global mass matrix,

$[K]=[B]^T[D][B]$ is the global stiffness matrix,

$[K_G]=[B_G]^T[D_G][B_G]$ is the geometric stiffness matrix and ω and Δ are the natural frequency and eigenvalue of the corresponding vectors.

where, $[B]$ and $[B_G]$ are the differential operators of the total and geometrical mid-plane strains respectively.By imposing (12)-(15) in the above governing equation, the equilibrium equation of the vibrated FG shallow shell panelis achieved and expressed in global form, as

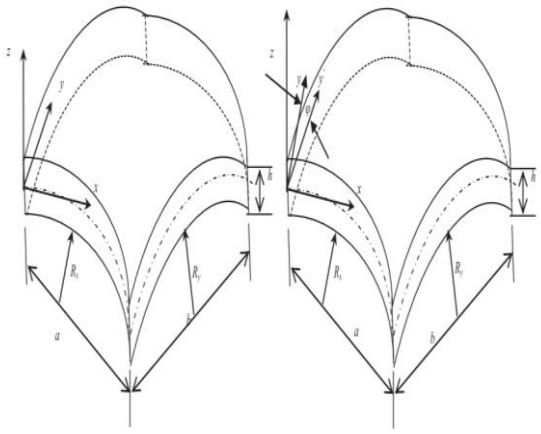

Fig. 7. (i) spherical curved shell form (ii) skew spherical curved shell form

IV. RESULT AND DISCUSSION

The free vibration characteristics of the spherical shell structure of the theoretical formulation model have presented by using HSDT and conjunction with the finite element method. The FG material properties, according to four parameters, power-law distribution in terms of volume fraction of constituents, are estimated by Voigt's rule mixture. In all numerical examples, material properties are listed in Table. I. To calculate the nondimensional frequency parameters, according to Refer to(16).

$$\left(\bar{\omega} = \omega(a^2/h)\sqrt{\rho_c/E_c}\right) \quad (16)$$

Table- I: Material properties of Strain less steel and Silicon nitrate [15]

Material's	Youngs modulus's (Gpa)	Poisson's ratio, μ	Mass density(kg/m3)
Si_3N_4	322.27×10^9	0.24	2370
SUS304	207.78×10^9	0.3177	8166

A. Convergence test and comparison study

To the effectiveness of the method, the convergence study gives great importance to determine the number of nodes required and uniform mesh size at which the natural frequencies converge. Therefore, based on the above analysis, the fig. 8 shows, the subsequent investigations carried out using a uniform mesh size of 6×6. The SUS304/ Si3N4 spherical shell (Rx = Ry = R) in rectangular form with all edges are supported conditions considered.

Table II. shows the comparisition study on the FGM constituents values are as follows Aluminum (Al) (E=70Gpa,ρ=2707kg/m^3,μ=0.3) and Silicon Carbide (Sic)(E=427Gpa,ρ=3210kg/m^3,μ=0.17).The position's ratio assumed to be constant (μ=0.3).

The frequencies of the first five modes for a Simply supported, for four different values of the thickness ratios (a/h = 5,20,50, and 200). The power-law distribution parameters FGM (u=1, v=0, w=2, φ=2), Geometrical parameters (R/a=5, a/b=1) with five skew angles (α=0^0, 15^0,30^0,45^0,60^0). the exact numerical solutions obtained by the present model are in excellent agreement with the available solutions reported in the literature. The theoretical formulations are developed by using the customized computer code in the MATLAB environment.

the examination of Some numerical examples implemented to show the accuracy of the present developed model.

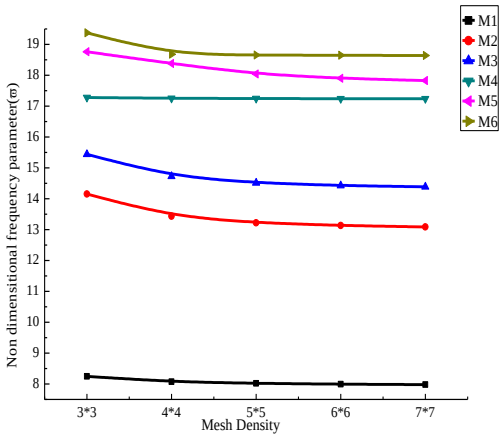

Fig.8 Dimensionless frequency parameter of a simply supported all edge of spherical shell

B. Numerical examples and discussion

Numerical investigations are presented in this section to check the performance of the present finite element procedure based on HSDT for Spherical shell structure. Choice of four-parameter power-law distributions parameters carried out for free vibration analysis of the FG spherical shell structure,

which is composed of two constituent's ceramic- rich (silicon nitride Si3N4) top surface, and metal-rich (stainless steel SUS304) bottom surface. The active material properties of FGM structures vary continuously in the thickness direction(ξ).

Examine the influence of the free vibration behavior of the FG spherical shell with the effects of the material composition. Four parameter Power-law Refer (3) and power-law material distribution parameters (u, v, w, φ).The significance of geometrical ratios and skew angles on the vibration characteristics of the non-dimensional frequenciespresented.

Table- II:**Shows the comparison of Non-dimensional frequency parameter for FG spherical (Aluminum (Al) and Silicon Carbide (Sic)), shell panels with different Thickness (a/h) ratios.**

FGM(u=1/v=0/w=2/φ=2) Power law distribution											
Skew angle(α)											
0				15^0		30^0		45^0		60^0	
a/h	mode	Mouli etal. [29]	Present	Mouli etal. [29]	Present	Mouli etal. [29]	Present	Mouli etal. [29]	Present	Mouli etal. [29]	Present
5	1	3.41	3.41	3.6408	3.6408	4.4156	4.4156	6.1069	6.1069	10.0314	10.0314
	2	6.8281	6.8281	7.0037	7.0037	7.6278	7.6278	8.923	8.923	11.624	11.624
	3	6.829	6.829	7.0591	7.0591	7.7858	7.7858	9.3418	9.3418	12.7402	12.7402
	4	7.4322	7.4322	7.3561	7.3561	8.0807	8.0807	9.9786	9.9786	14.4919	14.4919
	5	7.4328	7.4328	8.2882	8.2882	10.1929	10.1929	11.8894	11.8894	14.7162	14.7162
20	1	4.6859	4.6859	5.2709	5.2709	6.6948	6.6948	9.5462	9.5462	17.1977	17.1977
	2	9.8392	9.8392	10.1067	10.1067	11.8048	11.8048	15.6993	15.6993	26.1756	26.1756
	3	9.8399	9.8399	11.647	11.647	15.7501	15.7501	23.3829	23.3829	37.2351	37.2351
	4	15.1368	15.1368	15.8461	15.8461	18.1545	18.1545	23.9133	23.9133	44.4248	44.4248
	5	19.2254	19.2254	20.6338	20.6338	25.3188	25.3188	32.7678	32.7678	47.0353	47.0353
50	1	7.9556	7.9556	8.8234	8.8234	10.0229	10.0229	12.7876	12.7876	21.6786	21.6786
	2	11.9952	11.9952	12.8408	12.8408	14.7504	14.7504	19.3674	19.3674	33.2335	33.2335
	3	11.9964	11.9964	15.2141	15.2141	19.9778	19.9778	29.6364	29.6364	51.2778	51.2778
	4	16.9843	16.9843	19.1813	19.1813	22.5151	22.5151	29.9588	29.9588	56.5794	56.5794
	5	21.5536	21.5536	23.5513	23.5513	29.7915	29.7915	44.0315	44.0315	75.5599	75.5599
200	1	28.2112	28.2112	28.7029	28.7029	29.1911	29.1911	30.6427	30.6427	36.8841	36.8841
	2	29.7181	29.7181	30.3673	30.3673	31.2642	31.2642	34.2175	34.2175	47.0289	47.0289
	3	29.7252	29.7252	32.3829	32.3829	34.8612	34.8612	42.4027	42.4027	69.3334	69.3334
	4	32.0759	32.0759	34.6465	34.6465	36.668	36.6668	43.4188	43.4189	70.5579	70.5579
	5	35.0713	35.0713	36.9586	36.9586	41.9366	41.9366	55.7493	55.7493	101.8152	101.8152

Table- III: Variation of Non-dimensional frequency parameter under various boundary conditions

BCC	Mode	0^0	15^0	30^0	45^0	60^0
SSSS	1	7.2548	7.8844	9.9071	14.2829	25.0697
	2	16.6044	16.5355	18.6177	23.965	37.372
	3	16.6058	18.8812	24.1552	29.3097	38.4605
	4	22.3169	22.907	24.9905	30.7851	42.4492
	5	22.3199	23.0932	25.5662	33.9022	49.116
	6	25.2062	25.5742	27.8074	35.0576	49.6105
CCCC	1	12.2607	12.8913	15.1152	20.3394	33.4233
	2	22.7268	22.5697	24.7718	30.7707	45.8993
	3	22.7268	25.1269	30.6804	41.154	58.3686
	4	31.6662	32.0821	34.4734	42.2082	63.8333
	5	37.8218	39.499	44.384	50.0545	68.5847
	6	38.221	41.0425	45.2495	52.7604	72.1796
HHHH	1	7.7059	8.2973	10.2317	14.5065	25.2019
	2	16.6396	16.5832	18.6732	24.025	37.4552
	3	16.641	18.9024	24.1773	33.9488	49.5577
	4	25.2415	25.6125	27.8501	35.0349	60.2575
	5	31.0056	32.6789	38.352	45.2253	61.1479
	6	31.0134	33.8876	38.6175	48.3852	63.4311

C. Effect of boundary conditions with power law distribution

Table III. depicts the effect of general boundary conditions are considering supported (SSSS), clamped boundary condition (CCCC), and Hinged (HHHH) in all edges and FGM (u=1/v=1/w=2/φ=2) power-law distributions and following geometric values used for the analysis (a/h=10, R/a=5) presented here. The clamped boundary condition would also strengthen compared to the other boundary conditions. and thus, induces higher frequencies of vibration of the shell. similar trend mirrored for all the above cases.

D.Effect of curvature ratio with power law distribution

Tables IV to VI shows the effect of curvature ratio (R/a), on the variation of the non-dimensional frequency parameter with four-parameterpower-law distribution FGM (u=1/v=0/w=0/φ=5) and FG spherical shell made of Si3N4/SUS304/, is described with SSSS CCCC, and HHHH boundary conditions.

Tables IV-VI, respectively the frequency characteristics shown in three tables. For the above cases, five different values of curvature ratio (R/a = 5,10, 20 and 50,100) and Skew angles range from 0^0 to 60^0 are considered.

Tables IV and Villustrates the frequencies for the first six modes for simply supported and clamped boundary conditions, (a/h=10, a/b=1), respectively.it is observed that the frequencies in all six modes increase with rising the skew angle. Whereas for shells with curvature ratio increases, the natural frequencies gradually drop. The lower radii of curvature values present higher frequency values. For the reason that as the curvature ratio of any shell curved panel increases, the fundamental frequency decrease that leads to consistent approaches to flatness.

Table VI. shows the non-dimensional frequency rate of the first six modes observed for accelerating trend HHHH boundary condition, with rising skew angles. Descent flow of non-dimensional frequency parameters while increasing curvature ratios.

E.Effect of aspect ratio with power law distribution

The second example consists numerical results of Tables VII to IX illustrate the effect of the aspect ratio on the frequency responses of the FG spherical shell panel has analyzed. for three different boundary conditions, and following geometric quantiles are five different values of aspect ratio (a/b =1,1.5,2,2.5,3) and the a/h=5, R/a=5 and power-law distribution FGM(u=1/v=1/w=2/φ=2) with five skew angles 0^0,15^0,30^0,45^0,60^0. The detailed numerical results are shown.

Table VII. describe the variation of the fundamental natural frequencies with the power-law distribution. With askew angle for simply supported, it is noticed that the non-dimensional frequencies slowly improve as the skew angle increases from 0^0 to 30^0. Pronounced frequency increments occurring when the skew angle rises from 30^0 to 60^0. The result shows that the frequency parameter values are increasing with the aspect ratio. Because the large aspect ratios are comparatively stiffer, and it also prominent affect the structural design and vibration behavior of the structure.

Tables VIII and IX illustrate the first six frequency modes for Variation of Non-dimensional frequency parameter for clamped condition and hinged condition. The frequencies gradually increase as the aspect ratio increases. among them CCCC boundary condition exhibit higher frequency parameter values compared to the other boundary conditionstiffer, and it also prominent affect the structural design and vibration behavior of the structure.

F.Effect of thickness ratio with power law distribution

Tables X to XII demonstrate the effect of the thickness ratio on the frequency responses of the FG spherical shell SUS304/Si3N4 panel. With FGM (u=1/v=0/w=2/ φ=2) the following geometric parameters (a/b=1, R/a=5) and different thickness ratio values of (a/h=5,10,20,50,100,200) are presented. five skew angles 0^0 to 60^0, for three different boundary conditions.

Table X shows the frequencies in the first six modes for simply supported with the power-law distribution. The frequency parameters are showing the enhancing type of behavior with the increasing thickness ratio and skew angles. The modes of frequency increase first mode to the sixth mode, and orientation of the angle escalate 0^0 to 60^0. The frequency parameter is also uprising for all conditions.

Table XI and XII shows similar frequency characteristics shown for clamped and hinged boundary condition. Increment trends noticed at skew angles more than 30^0.

Table- IV, V, VI: Variation of Non-dimensional frequency parameter for simply supported condition with FG spherical (SUS304/(Si3N4), shell panel with different curvature ratios(R/a).

Table-IV: (R/a) ratios under SSSS boundary condition

R/a	Mode	0^0	15^0	30^0	45^0	60^0
5	1	8.1595	8.8732	11.1613	16.1079	28.3267
	2	18.6892	18.6176	20.9813	27.0447	42.2906
	3	18.6909	21.2662	27.2484	33.2533	43.608
	4	25.326	25.9952	28.3574	34.9273	48.1235
	5	25.3295	26.2059	29.004	38.3086	55.7371
	6	28.4067	28.8306	31.3759	39.6053	56.1237
10	1	7.8641	8.6022	10.9473	15.9605	28.2393
	2	18.5668	18.4947	20.874	26.9642	42.2471
	3	18.5684	21.16	27.1748	33.2758	43.6297
	4	25.3446	26.0138	28.3771	34.9562	48.1514
	5	25.3481	26.2236	29.0113	38.2442	55.8191
	6	28.3248	28.7494	31.3003	39.532	56.0241
20	1	7.7869	8.5314	10.891	15.9204	28.2121
	2	18.5327	18.4605	20.8432	26.9388	42.2255
	3	18.5343	21.1295	27.1509	33.2877	43.6448
	4	25.3539	26.0233	28.3873	34.9696	48.1688
	5	25.3574	26.2329	29.0194	38.2211	55.8276
	6	28.2994	28.7241	31.2759	39.5076	56.0112
50	1	7.7642	8.5105	10.8738	15.9072	28.201
	2	18.521	18.4487	20.8321	26.9284	42.2127
	3	18.5226	21.1185	27.1408	33.295	43.655

Table-V: (R/a) ratios under CCCC boundary condition

R/a	Mode	0^0	15^0	30^0	45^0	60^0
5	1	13.8005	14.5117	17.0219	22.9304	37.7785
	2	25.6466	25.4698	27.9691	34.7841	52.0085
	3	25.6466	28.3676	34.6729	46.5723	66.1957
	4	35.7704	36.245	38.967	47.7913	72.2593
	5	42.7799	44.688	50.3542	56.7375	77.89
	6	43.2094	46.4147	51.2344	59.7402	81.9194
10	1	13.4325	14.1623	16.7251	22.7098	37.6406
	2	25.547	25.3637	27.8657	34.6918	51.93
	3	25.547	28.2819	34.6043	46.4901	66.1208
	4	35.6867	36.1587	38.8799	47.7353	72.3129
	5	42.7131	44.6226	50.4173	56.7811	77.8128
	6	43.1259	46.337	51.172	59.6581	81.8507
20	1	13.338	14.0726	16.6489	22.6529	37.604
	2	25.5172	25.3326	27.835	34.6629	51.9022
	3	25.5172	28.2548	34.58	46.4631	66.0938
	4	35.66	36.1314	38.8524	47.7101	72.3438
	5	42.6885	44.5978	50.4358	56.8014	77.7688
	6	43.0992	46.3111	51.1465	59.6358	81.8262
50	1	13.3108	14.0468	16.6268	22.6361	37.5924
	2	25.5059	25.3209	27.8233	34.6512	51.8891
	3	25.5059	28.2438	34.5686	46.4515	66.0809

	4	25.3595	26.029	28.3935	34.9773	48.1803
	5	25.363	26.2386	29.0254	38.2101	55.8154
	6	28.2892	28.7139	31.2655	39.4969	56.0222
100	1	7.7606	8.5071	10.8709	15.9046	28.1982
	2	18.5186	18.4463	20.8296	26.9257	42.2085
	3	18.5202	21.1161	27.1381	33.2975	43.6586
	4	25.3614	26.0309	28.3956	34.9798	48.1843
	5	25.3648	26.2406	29.0277	38.2069	55.8091
	6	28.2866	28.7113	31.2628	39.494	56.0283

	4	35.6488	36.1202	38.8411	47.6959	72.3636
	5	42.6765	44.5856	50.4415	56.813	77.7408
	6	43.0881	46.2998	51.133	59.6286	81.8147
100	1	13.3067	14.0429	16.6234	22.6333	37.5903
	2	25.5032	25.3182	27.8206	34.6483	51.8854
	3	25.5032	28.2409	34.5653	46.4484	66.0772
	4	35.6459	36.1173	38.8382	47.6913	72.3704
	5	42.673	44.5819	50.4424	56.8167	77.7311
	6	43.0852	46.2967	51.1289	59.6272	81.8114

Table-VI: (R/a) ratios under HHHH boundary condition

R/a	Mode	0^0	15^0	30^0	45^0	60^0
5	1	8.8893	9.5456	11.7044	16.5081	28.5947
	2	18.7701	18.7169	21.0885	27.151	42.3907
	3	18.7716	21.3199	27.2825	38.4079	56.1583
	4	28.5062	28.9328	31.4797	39.5807	68.1774
	5	34.9913	36.8821	43.3204	51.1673	69.2468
	6	35.0249	38.2895	43.6437	54.8458	71.9539
10	1	8.1288	8.8446	11.1427	16.1085	28.3459
	2	18.6011	18.5348	20.9154	27.0035	42.2765
	3	18.6027	21.1841	27.1884	38.2856	56.0524
	4	28.3712	28.7961	31.3459	39.5271	68.1837
	5	34.9133	36.809	43.2587	51.0977	69.272
	6	34.917	38.1899	43.5659	54.8362	71.8474
20	1	7.8982	8.6336	10.9749	15.9875	28.2656
	2	18.5509	18.4806	20.8632	26.957	42.2369
	3	18.5525	21.1432	27.1587	38.2433	56.0126
	4	28.3267	28.7511	31.3014	39.5075	68.1815
	5	34.8777	36.7841	43.2363	51.071	69.2899
	6	34.8894	38.1549	43.5376	54.8423	71.8049
50	1	7.8139	8.5564	10.9128	15.9409	28.2317
	2	18.5319	18.4602	20.843	26.938	42.2188
	3	18.5335	21.1273	27.1464	38.224	55.993
	4	28.3075	28.7316	31.2819	39.4982	68.1784
	5	34.8607	36.7728	43.2256	51.0576	69.3022
	6	34.878	38.1385	43.5241	54.8493	71.7829
100	1	7.7951	8.5391	10.8987	15.9298	28.2228
	2	18.5275	18.4554	20.8381	26.9332	42.2137
	3	18.5291	21.1235	27.1433	38.2186	55.9871
	4	28.3023	28.7264	31.2766	39.4954	68.1771
	5	34.856	36.7697	43.2225	51.0535	69.3065
	6	34.8749	38.1338	43.5202	54.8522	71.7761

Table-VII: (a/b) ratios under SSSS boundary condition

a/b	Mode	0^0	15^0	30^0	45^0	60^0
5	1	5.7832	6.1551	7.4093	10.149	16.4495
	2	10.296	10.5675	11.5274	13.5194	17.7337
	3	10.2974	10.6524	11.7823	14.1991	19.5705
	4	12.4627	12.3156	13.438	16.4416	22.7025
	5	12.4637	13.8485	15.962	18.1586	23.5558
	6	14.6075	14.9162	16.9025	22.1652	29.7113
10	1	8.7493	9.2233	10.8367	13.0822	16.1514
	2	10.3129	10.5758	11.4255	14.4034	22.739
	3	14.8484	15.3831	17.1976	20.9389	28.4447
	4	15.468	15.9442	17.5393	21.1489	28.511
	5	18.6116	18.9673	20.1997	22.8512	30.0434
	6	20.6398	21.1333	22.7244	25.9653	32.8987
20	1	10.3194	10.532	11.2	12.4246	14.4644
	2	12.4448	13.0797	15.2538	20.0984	28.765
	3	17.9209	18.5898	20.8499	24.2538	31.4612
	4	20.637	20.946	21.999	25.7646	36.986
	5	20.653	21.2952	23.5075	28.2407	38.2955
	6	23.0793	23.7602	25.9268	30.3184	39.7546
50	1	10.3226	10.4999	11.0476	12.0192	13.5621
	2	16.6249	17.4449	20.2535	23.8835	27.4354
	3	20.6595	20.9632	21.9543	26.5005	41.0208
	4	21.5121	22.3313	25.112	31.2112	41.6013
	5	25.8039	26.6442	29.4697	34.9583	45.2808
	6	27.791	28.588	31.2314	35.7258	48.8631
100	1	10.3244	10.4767	10.9425	11.7546	13.0166
	2	20.6632	20.9428	21.8322	23.4993	26.4443
	3	21.1191	22.1321	25.5951	33.2566	40.9791
	4	25.4832	26.4711	29.8332	35.2322	50.5276
	5	30.9693	31.4171	32.6128	37.2392	50.9167
	6	31.0842	31.994	35.4394	42.8158	54.3551

Table-VII, VIII and IX: Variation of non-dimensional frequency responses with skew angle (α) for FG spherical shell (SUS304/Si3N4) panel for different aspect ratios(a/b).

Table-VIII: (a/b) ratios under CCCC boundary condition

a/b	Mode	0^0	15^0	30^0	45^0	60^0
5	1	8.8081	9.2064	10.5665	13.5559	20.3344
	2	15.1719	15.0371	16.1793	19.2491	26.5813
	3	15.1719	16.5252	19.4987	23.1289	29.4766
	4	19.919	19.6581	20.5361	24.8215	32.8185
	5	19.919	20.5161	21.6284	25.318	37.829
	6	20.3675	21.2588	24.0197	29.2839	39.4421
10	1	12.7704	13.3237	15.2007	19.2854	28.4888
	2	17.9687	18.5113	20.3743	24.4824	33.8373
	3	22.9911	23.4205	24.9741	28.5828	37.0965
	4	24.0548	25.1109	27.3669	31.4131	41.2999
	5	25.567	25.8417	28.6288	35.9897	48.6611
	6	27.6275	28.6193	31.8757	38.6576	49.0154
20	1	17.4387	18.1694	20.6443	26.0239	38.1852
	2	21.6496	22.3581	24.7632	30.0128	41.9662
	3	26.7273	27.3531	29.5185	34.3773	45.7153
	4	28.3553	29.0063	31.2859	36.4409	48.5104
	5	33.2734	34.587	38.5906	44.2202	56.1039
	6	35.801	37.0181	39.8496	45.5064	57.0656

Table-IX: (a/b) ratios under HHHH boundary condition

a/b	Mode	0^0	15^0	30^0	45^0	60^0
5	1	5.9072	6.2717	7.5068	10.2225	16.5003
	2	12.4582	12.3155	13.4385	16.4407	23.5516
	3	12.4592	13.8363	16.8789	21.471	27.051
	4	17.93	18.0399	19.0909	22.1785	29.8667
	5	18.4713	18.2926	19.125	22.8874	34.8976
	6	18.4714	19.5931	21.9185	26.2786	36.2695
10	1	8.8343	9.3043	10.9069	14.4586	22.778
	2	14.8595	15.3941	17.2089	21.1565	30.0536
	3	21.0959	22.0483	23.5298	26.953	35.0236
	4	21.6577	22.1776	24.8005	28.7235	38.232
	5	23.1498	23.3571	25.7373	32.2356	41.9301
	6	24.3454	25.1272	27.6398	33.6465	43.7713
20	1	12.5078	13.1401	15.3069	20.1412	31.4891
	2	17.9394	18.6082	20.8683	25.783	37.0051
	3	25.5191	26.1277	28.2378	32.9834	44.0814
	4	25.6167	26.2474	28.4495	33.3947	44.8479
	5	29.6972	30.6271	33.489	39.0482	49.4467
	6	30.9413	32.2413	36.2565	41.3063	50.9772

50	1	22.3722	23.2845	26.3739	33.0956	48.3317
	2	25.8568	26.7354	29.7175	36.2373	51.1426
	3	30.8821	31.6926	34.4757	40.6673	55.0277
	4	31.7374	32.5695	35.4204	41.742	56.4424
	5	39.5202	40.2735	42.9838	49.2693	63.8587
	6	42.4532	43.0424	45.301	50.7194	64.3654
100	1	27.4183	28.5139	32.2258	40.3106	58.6562
	2	30.3728	31.4296	35.0188	42.8773	60.8623
	3	35.3061	36.303	39.715	47.269	64.6982
	4	35.5511	36.5563	39.9883	47.5752	65.1883
	5	42.6764	43.6347	46.9519	54.4237	72.1211
	6	45.8049	46.6176	49.5032	56.1805	72.2195

50	1	16.6747	17.4928	20.2963	26.5338	41.0442
	2	21.5333	22.3523	25.1325	31.2312	45.2959
	3	28.5877	29.3856	32.1067	38.1001	50.6459
	4	29.7861	30.5863	33.3363	39.4611	51.909
	5	35.1859	36.1327	39.1974	45.2062	53.6732
	6	37.1813	37.8976	40.4914	46.4918	55.8732
100	1	21.1603	22.1716	25.6301	33.2848	50.5074
	2	25.5048	26.4925	29.854	37.2561	50.9363
	3	31.9658	32.9208	36.1718	43.3341	54.3695
	4	34.3046	35.2955	38.6883	46.2018	55.2704
	5	40.0165	40.9343	44.1032	49.9764	60.0647
	6	40.0737	41.088	44.3515	50.8968	61.3982

Table-X, XI and XII: Variation of non-dimensional frequency responses with skew angle (α) for FG spherical shell (SUS304/Si3N4) panel for different thickness ratios(a/h).

Table-X:(a/h) ratios under SSSS boundary condition

a/h	Mode	0^0	15^0	30^0	45^0	60^0
5	1	6.4844	6.9049	8.323	11.4229	18.5641
	2	11.5826	11.8874	12.9643	15.1959	19.9018
	3	11.5841	11.9827	13.251	15.9591	21.9511
	4	14.0165	13.8516	15.1239	18.5286	25.4194
	5	14.0176	15.5843	17.9259	20.3757	26.6041
	6	16.4121	16.7573	19.043	25.0139	33.2075
10	1	7.3799	8.0315	10.1158	14.6199	25.7786
	2	16.9293	16.87	19.0332	24.5764	38.5553
	3	16.9308	19.2807	24.7506	30.4896	39.9826
	4	23.2212	23.8347	26.0006	32.0239	44.1242
	5	23.2243	24.0279	26.5918	34.8833	51.0689
	6	25.7825	26.1765	28.5179	36.0664	51.307
20	1	8.6299	9.665	12.3353	17.7308	32.0437
	2	18.5791	18.9718	22.0947	29.3632	48.7951
	3	18.5804	21.8381	29.3897	43.5167	68.8255
	4	28.6903	29.8425	33.9481	44.6223	80.063
	5	36.3626	38.9406	47.5546	60.6264	82.72
	6	36.384	40.943	48.8001	61.1171	88.4353
50	1	13.9963	15.6268	18.0422	23.4226	40.272
	2	22.0713	23.5772	27.2709	36.0203	61.8359
	3	22.0733	27.8554	37.0421	55.3216	94.7245
	4	31.7841	35.5722	41.9003	55.7185	105.6497
	5	40.5114	44.1939	55.8907	81.9358	138.4041
	6	40.5287	50.8849	61.1837	82.4583	153.7145
100	1	25.0154	26.4683	28.013	32.3094	48.5938
	2	30.4081	32.1824	35.1573	43.4852	72.1091
	3	30.4132	37.3492	44.9598	63.2088	113.6709
	4	38.151	43.8119	49.5143	64.8411	119.3339
	5	46.1815	50.4456	62.4914	91.6224	174.0035
	6	46.2252	60.508	70.188	96.2225	176.2786
200	1	48.415	49.4068	50.3863	53.3161	65.8797
	2	51.5386	52.856	54.7169	60.752	86.1595
	3	51.5504	56.9402	62.0318	77.1118	129.1558
	4	56.433	61.5489	65.648	79.0604	131.7446
	5	62.477	66.2374	76.1901	103.2362	191.4373
	6	62.6028	75.4011	83.7805	109.7603	197.622

Table-XI:(a/h) ratios under CCCC boundary condition

a/h	Mode	0^0	15^0	30^0	45^0	60^0
5	1	9.8917	10.3416	11.8788	15.2616	22.9422
	2	17.1328	16.9776	18.2734	21.7593	30.0796
	3	17.1328	18.6743	22.0621	25.8536	32.8457
	4	22.2908	22.0048	22.9813	28.0444	37.1058
	5	22.2908	23.1639	24.4238	28.6895	42.683
	6	22.9971	23.7713	26.8181	32.6119	44.5199
10	1	12.5081	13.1545	15.4384	20.8276	34.4294
	2	23.3006	23.1416	25.4306	31.6791	47.5168
	3	23.3006	25.7866	31.5589	42.4942	60.5756
	4	32.5563	32.9951	35.4988	43.6041	66.2571
	5	38.9964	40.7494	46.1608	52.0223	71.3571
	6	39.3798	42.3202	46.7691	54.6035	75.0671
20	1	14.7818	15.497	18.105	24.6732	43.2262
	2	27.3882	27.3177	30.5203	39.4454	63.961
	3	27.3882	30.5148	38.1578	55.2353	86.2766
	4	39.2849	40.1925	44.344	55.6097	99.3261
	5	49.1165	51.7281	60.8825	75.2541	112.6996
	6	49.4617	53.4516	61.8101	82.2723	132.8863
50	1	21.659	22.2569	24.5859	31.1881	52.6487
	2	32.2044	32.4266	36.6639	48.6986	83.6986
	3	32.2044	35.5684	44.4682	65.6805	123.1938
	4	45.3695	47.1371	54.1595	72.5866	125.0755
	5	58.6788	62.3338	75.4413	105.7947	175.2543
	6	59.1674	63.9592	79.6443	107.2611	192.4532
100	1	35.8457	36.2788	38.0199	43.3516	63.6352
	2	39.8613	40.3711	44.7356	57.5838	98.6171
	3	39.8613	42.6711	51.0196	72.9032	139.4706
	4	51.7713	53.8817	62.1117	84.6176	151.6439
	5	65.0653	69.0017	83.5539	120.8787	228.2105
	6	66.3674	71.1497	88.5451	126.4659	228.7672
200	1	60.2542	61.2149	65.2091	72.2293	88.1884
	2	60.2542	61.7608	67.329	76.5954	116.5011
	3	64.4909	65.066	67.6793	86.1092	151.9582
	4	68.92	71.2878	79.2078	100.7438	173.5842
	5	79.0797	82.543	95.888	132.8021	249.7201
	6	85.1415	88.4828	102.6693	142.6778	265.215

Table-XII:(a/h) ratios under HHHH boundary condition

a/h	Mode	0^0	15^0	30^0	45^0	60^0
5	1	6.7532	7.1602	8.5433	11.597	18.6846
	2	14.001	13.8461	15.1197	18.5159	26.5472
	3	14.0021	15.5503	18.9769	23.9762	30.0648
	4	20.2139	20.3408	21.3974	25.0341	33.7387
	5	20.6654	20.4715	21.5346	25.7478	38.069
	6	20.6654	21.9005	24.4525	29.1971	40.4516
10	1	8.1251	8.7192	10.6758	15.0424	26.0785
	2	17.0212	16.9804	19.1508	24.6932	38.664
	3	17.0226	19.3435	24.788	35.0005	51.3265
	4	25.9017	26.298	28.64	36.0421	62.3003
	5	31.8085	33.542	39.4473	46.6906	63.5339
	6	31.8596	34.8497	39.7611	50.3276	65.8888
20	1	10.6233	11.4299	13.7191	18.7568	32.7424

	2	18.8955	19.317	22.4345	29.6975	49.1142
	3	18.8964	22.0629	29.5262	43.8136	69.1062
	4	29.0314	30.1732	34.2596	44.6989	82.7923
	5	36.4902	39.0583	47.6425	60.9111	93.4627
	6	36.6339	41.162	49.0215	67.0084	116.1053
50	1	19.903	20.6762	22.421	27.0464	42.7481
	2	23.328	24.7545	28.4542	37.2625	63.0277
	3	23.3282	28.6402	37.5172	55.5995	95.6122
	4	33.0556	36.6345	42.8763	56.6675	105.7956
	5	40.9651	44.7529	56.2769	82.5848	139.0456
	6	41.5789	51.5069	61.8274	82.7114	153.8556
100	1	33.4761	34.8701	37.4994	41.2907	55.5616
	2	33.4762	36.1085	38.1561	46.9278	75.5054
	3	35.6603	39.2035	46.2803	64.0265	115.9655
	4	41.4961	46.4327	52.2142	67.4578	119.7053
	5	47.4341	52.158	63.604	92.3269	175.5296
	6	50.1616	62.1188	71.7893	97.8537	176.6544
200	1	57.6026	58.3118	61.1165	69.1173	83.8557
	2	57.6026	61.036	65.4103	71.6169	95.868
	3	59.6508	62.0571	65.6407	79.6989	132.9465
	4	63.8713	67.9257	74.4335	87.209	135.8121
	5	65.6328	73.2623	80.309	105.4379	192.5408
	6	74.9892	79.5408	88.3154	114.4667	201.7579

V. SUMMARY AND CONCLUSIONS

The comprehensive examination of free vibration characteristics of the FG rectangular spherical shell (Si3N4/SUS304) is studied. The FGM material composition, the top surface ceramic-rich, and another face metal-rich considered. To Employed Voigt's micromechanical model, Material properties continuously vary through the specified direction. To Assesses the precision of the present formulation based on HSDT conjunction with the finite element method. The non-dimensional frequency parameters of the shell panel result seen good agreement with the authors' solutions. The vibration responses determine fundamental frequencies to representing all essential characteristics of the structural elements for the technical design. The numerical results have shown the significance of geometrical parameters of the shell curvature ratio, aspect ratio, and thickness ratio, and the importance of volume fraction profiles, choice of material distribution parameters (u, v, w, φ). Effect of four-parameter power-law distribution with skew angle (α) and various boundary conditions are simply supported, clamped, and hinged in all edges on the vibration responses examined. The studies of free vibration analysis on the spherical shell following conclusions points are derived here.

- Curvature ratio increases, the frequency responses are decreasing trend. When the other geometrical parameters and power-law distribution parameters kept constant. A similar pattern follows under three different boundary conditions. The smaller curvature ratio exhibits maximum frequency responses.
- The frequency responses are consistently rising, with thickness ratio for all boundary conditions. The non-dimensional frequency parameters found for CCCC, and SSSS, boundary conditions are exhibit the highest and lower responses.
- Various aspect ratios (a/b) with skew angles and Four parameter power-law distribution for SSSS, CCCC, HHHH, boundary conditions. The nondimensional frequency parameters increase with increasing aspect ratios for shells.
- In all cases, the three boundary conditions exhibit a detectable effect on the frequency parameter of the spherical shell. The most obvious the frequency parameters are increasing trend observed for all the FG rectangular shell with clamped boundary conditions.
- Variations of the ceramic volume fractions of through the thickness direction, for different values of the power-law exponent. Selecting suitable various parameters on power-law distributions (u, v, w). the impression is possible to study the effect of the different species of material profiles, including classic, symmetric, asymmetric, on the mechanical behavior of FGM structures.
- The response of fundamental non-dimensional frequency parameter values for a given skew angle varied from 0^0 to 60^0.at the interval of 15^0.the parameter values show 0^0 for minimum and at 45^0 exhibits sharp escalating trend seen. For different skew angles under various boundary conditions, frequency responses are increasing trend with skew angles increases.

REFERENCES

1. M. Koizumi, "FGM activities in Japan," vol. 8368, pp. –4, 1997.
2. C. T. Loy, K. Y. Lam, and J. N. Reddy, "Vibration of functionally graded cylindrical shells," Int. J. Mech. Sci., vol. 41, no. 3, pp. 309–324, 1999.
3. S. C. Pradhan, C. T. Loy, K. Y. Lam, and J. N. Reddy, "Vibration characteristics of functionally graded cylindrical shells under various boundary conditions," vol. 61, pp. 111–129, 2000.
4. J.N.Reddy, "Analysis of functionally graded plates," Int. J. Numer. Methods Eng., vol. 47, no. June 1999, pp. 663–684, 2000.
5. Lee YS, Yang MS, Kim HS. A study on the free vibration of the joined cylindrical-spherical shell structures. Civil-Comp Press; 2000.
6. J. N. Reddy and Z. Cheng, "Frequency correspondence between membranes and functionally graded spherical shallow shells of polygonal planform," vol. 44, pp. 967–985, 2002.
7. B.P. Patel, S.S., ZGupta,M.S.Loknath, C.P.Kandu. Free vibration analysis of functionally gradedelliptical cylindrical shells using higher-order theory. Composit structures 2005;69:259–270.
8. X. X. Hu, T. Sakiyama, H. Matsuda, and C. Morita, "Vibration analysis of rotating twisted and open conical shells," Int. J. Solids Struct., vol. 39, no. 25, pp. 6121–6134, 2002.
9. Y. Xiang, Y. F. Ma, S. Kitipornchai, C. W. Lim, and C. W. H. Lau, "Exact solutions for vibration of cylindrical shells with intermediate ring supports," Int. J. Mech. Sci., vol. 44, no. 9, pp. 1907–1924, 2002.
10. J. Woo, S. A. Meguid, J. C. Stranart, and K. M. Liew, "Thermomechanical postbuckling analysis of moderately thick functionally graded plates and shallow shells," Int. J. Mech. Sci., vol. 47, no. 8, pp. 1147–1171, 2005.
11. E. Artioli and E. Viola, "Free vibration analysis of spherical caps using a G.D.Q. numerical solution," J. Press. Vessel Technol. Trans. ASME, vol. 128, no. 3, pp. 370–378, 2006.
12. R. A. Arciniega and J. N. Reddy, "Large deformation analysis of functionally graded shells," Int. J. Solids Struct., vol. 44, no. 6, pp. 2036–2052, 2007.
13. X. Zhao, K.M. Liew, T.Y. Ng, Vibration analysis of laminated composite cylindrical panels via a mesh-free approach, International Journal of Solids and Structures 40 (2003) 161–180.
14. X. Zhao, K.M. Liew, T.Y. Ng, The element-free kp-Ritz method for free vibration analysis of conical shell panels, Journal of Sound and Vibration 295 (2006) 906–922.
15. X. Zhao, Y. Y. Lee, and K. M. Liew, "Free vibration analysis of functionally graded plates using the element-free kp-Ritz method," J. Sound Vib., vol. 319, no. 3–5, pp. 918–939, 2009.
16. F. Tornabene and E. Viola, "Vibration analysis of spherical structural elements using the GDQ method," Comput. Math. with Appl., vol. 53, no. 10, pp. 1538–1560, 2007.

17. F. Tornabene and E. Viola, "2-D solution for free vibrations of parabolic shells using generalized differential quadrature method," Eur. J. Mech. A/Solids, vol. 27, no. 6, pp. 1001–1025, 2008.
18. F. Tornabene, "Free vibration analysis of functionally graded conical, cylindrical shell and annular plate structures with a four-parameter power-law distribution," Comput. Methods Appl. Mech. Eng., vol. 198, no. 37–40, pp. 2911–2935, 2009.
19. E. Viola and F. Tornabene, "Free vibrations of three parameter functionally graded parabolic panels of revolution," Mech. Res. Commun., vol. 36, no. 5, pp. 587–594, 2009.
20. F. Tornabene and E. Viola, Free vibrations of four-parameter functionally graded parabolic panels and shells of revolution, vol. 28, no. 5. 2009.
21. F. Tornabene and A. Ceruti, "Mixed static and dynamic optimization of four-parameter functionally graded completely doubly curved and degenerate shells and panels using GDQ method," Math. Probl. Eng., vol. 2013, 2013.
22. M. H. Yas and B. Sobhani Aragh, "Three-dimensional analysis for thermoelastic response of functionally graded fiber reinforced cylindrical panel," Compos. Struct., vol. 92, no. 10, pp. 2391–2399, 2010.
23. H. Shen and Z. Wang, "Assessment of Voigt and Mori – Tanaka models for vibration analysis of functionally graded plates," Compos. Struct., vol. 94, no. 7, pp. 2197–2208, 2012.
24. A. M. A. Neves et al., "Free vibration analysis of functionally graded shells by a higher-order shear deformation theory and radial basis functions collocation, accounting for through-the-thickness deformations," Eur. J. Mech. A/Solids, vol. 37, pp. 24–34, 2013.
25. S. K. P. Vishesh Ranjan Kar, "Free vibration responses of temperature dependent functionally graded curved panels under thermal environment," pp. 2006–2024, 2015.
26. A. Kumar, A. Chakrabarti, and P. Bhargava, "Vibration analysis of laminated composite skew cylindrical shells using higher order shear deformation theory," JVC/Journal Vib. Control, vol. 21, no. 4, pp. 725–735, 2015.
27. Q. Wang, D. Shi, Q. Liang, and F. Pang, "moderately thick doubly-curved panels and shells of," vol. 0, pp. 1–30, 2016.
28. D. Punera and T. Kant, "Free vibration of functionally graded open cylindrical shells based on several refined higher order displacement models," Thin-Walled Struct., vol. 119, 2017.
29. C. M. Badiganti and R. Koona, "Harmonic frequency analysis of skewed functionally graded flat and spherical shallow shells," Results Phys., vol. 10, no. June, pp. 987–992, 2018.
30. B. C. Mouli, V. R. Kar, K. Ramji, and M. Rajesh, "Free vibration of functionally graded conical shell," Mater. Today Proc., vol. 5, no. 6, pp. 14302–14308, 2018.
31. Cook, R. D. Malkus, D. S. Plesha, M. E., Witt, R. J., (2009). Concepts and applications of finite element analysis. John Wiley & Sons (Singapore).
32. Pandya, B.N., Kant, T. (1988a). Higher-order shear deformable theories for flexure of sandwich plates-Finite element evaluations. International Journal of Solids and Structures 24(12): 1267-1286.
33. Pandya, B.N., Kant, T. (1988b). Finite element analysis of laminated composite plates using a Higher-order displacement model. Composite Science and Technology 32: 137-155.

AUTHORS PROFILE

Raparthi Srilakshmi, Research Scholar in the Department ofMechanical Engineering, Andhra University has published paper on conditon monitoring. She has Diploma in Polytechnic, BE Mechanical, and M.Tech in Machine Design. She is interested in the areas of FEA, Composites, Solid Mechanics, Vibration Analysis, Signal Analysis, Condition Monitoring and SHM.

Prof. Ch. Ratnam, Professor and Head of the Department in the Department of Mechanical Engineering, Andhra University. He has books published on Fluid Mechanics & Machinery and Geometrical Drawing. He also received an award for best paper published in IEI Journal for the year 2003-2004 and hasover 60 papers in National and International journals. He has ample knowledge in Mechanical Engineering and Science, Vibration and Structural Health Monitoring, Engineering Optimization, Finite Element Analysis, Computer Aided Design and Design of Engineering.

Chandra Mouli Badiganti, Assoc. Professor in the Department ofMechanical Engineering of RISE Krishna SaiPrakasam Group ofInstitution has publishedaround 11 papers in various reputed journals. He has teaching experience in Strength of Materials, Composites, Engineering Drawing, Production Engineering.